Morphology of the radiodontan *Lyrarapax* from the early Cambrian Chengjiang biota

Peiyun Cong,[1] Allison C. Daley,[2,3] Gregory D. Edgecombe,[4] Xianguang Hou,[1] and Ailin Chen[1,5]

[1]Yunnan Key Laboratory for Palaeobiology, Yunnan University, Kunming 650091, China ⟨cong@ynu.edu.cn⟩ ⟨xghou@ynu.edu.cn⟩
[2]Department of Zoology, University of Oxford, The Tinbergen Building, South Parks Road, Oxford OX1 3PS, UK ⟨allison.daley@zoo.ox.ac.uk⟩
[3]Oxford University Museum of Natural History, Parks Road, Oxford OX1 3PW, UK
[4]Department of Earth Sciences, The Natural History Museum, Cromwell Road, London SW7 5BD, UK ⟨g.edgecombe@nhm.ac.uk⟩
[5]Research Center of Paleobiology, Yuxi Normal University, Yuxi, Yunnan 653100, China ⟨ailinchen@yxnu.net⟩

Abstract.—The recently described radiodontan *Lyrarapax unguispinus* Cong et al., 2014 from the Chengjiang biota (Cambrian Series 2, Stage 3) highlighted a new morphological type of frontal appendage and unique mouth structures, a functional combination reinforcing the diversification of feeding strategies of radiodontans during the early Cambrian. Here we describe *Lyrarapax trilobus* n. sp. from the same fossil Konservat-Lagerstätte. The new species differs from *L. unguispinus* in the morphology and distribution of endites on the frontal appendage and the strengthening structure of the body flaps. The two species resemble each other in body shape (pattern of flap size), neck segment number, cephalic plates, and most importantly a mouth characterized by concentric wrinkled furrows. The latter confirms that a soft mouth without sclerotized plates is a real feature of *Lyrarapax* and supports the idea that oral structures provide valid diagnostic characters within Radiodonta.

Introduction

Radiodontans such as *Anomalocaris* Whiteaves, 1892, *Peytoia* Walcott, 1911, and *Hurdia* Walcott, 1912 are icons of the Cambrian explosion. They have been the focus of much recent research because of their importance in understanding arthropod evolution, early animal ecology, and the mechanisms by which exceptional fossils come to be preserved. A few dozen species classified into 14 genera have been described worldwide primarily based on the morphology of frontal appendages, most from Cambrian sites of exceptional preservation, so-called Burgess Shale-type biotas. Foremost among these are the Burgess Shale in Canada (Whittington and Briggs, 1985; Collins, 1996; Daley and Budd, 2010; Daley et al., 2009, 2013a; Daley and Edgecombe, 2014); the Chengjiang (Chen et al., 1994; Hou et al., 1995; Cong et al., 2014) and Guanshan biotas (Wang et al., 2013) in Yunnan, China; the Emu Bay Shale in South Australia (Nedin, 1995; Paterson et al., 2011; Daley et al., 2013b); and Sirius Passet in North Greenland (Daley and Peel, 2010; Vinther et al., 2014). Radiodontans are not, however, confined to the lower and middle Cambrian, having sporadic records in the upper Cambrian (Lerosey-Aubril et al., 2014), the Ordovician (Van Roy and Briggs, 2011), including the largest known taxon at 2 m long (Van Roy et al., 2015), as well as the Devonian (Kühl et al., 2009). A range of feeding ecologies including apex predation, generalized predation, and filter feeding has recently been documented for the group based on the varied morphologies of appendages and mouthparts (Daley and Budd, 2010; Daley and Bergström, 2012; Vinther et al., 2014; Van Roy et al., 2015).

Radiodontans from the Chengjiang Konservat-Lagerstätte were first described in the mid-1990s and their diversity and unusual morphology inspired the first serious attempts to place the group within the tree of life (Chen et al., 1994; Hou et al., 1995). Radiodontans and other Cambrian predators such as *Opabinia* Walcott, 1912, and *Kerygmachela* Budd, 1993, were regarded either as mostly closely allied to cycloneuralian worms (Hou et al., 1995) or to arthropods (Chen et al., 1994). More recent collections in China have allowed new Cambrian taxa with distinctive morphologies to be identified (Huang et al., 2012; Liu, 2013; Wang et al., 2013; Cong et al., 2014). Among these, the most complete and informative is *Lyrarapax unguispinus* Cong et al., 2014, a taxon described from three whole-body specimens that exhibit a diagnostic combination of a short frontal appendage with one especially enlarged proximal endite bearing a row of pectinate spines; a pronounced, four-segmented neck region; and a hypertrophied first pair of body flaps. One specimen preserved traces of the brain, allowing for an appraisal of the segmental alignment of cephalic structures such as the frontal appendage (Cong et al., 2014) and the dorsal plate (Ortega-Hernández, 2015). The mouth apparatus was preserved in just one specimen, and this rarity coupled with its peculiar morphology (composed of concentric folds rather than overlapping, tooth-bearing plates as in other Radiodonta) did not allow for a determination of whether distinctive characters were taphonomically altered or of taxonomic value. Here we document new material of *Lyrarapax*, describing a new species from Chengjiang that allows the taxonomic status of various characters to be appraised.

663

Stratigraphy, material, and methods

The stratum that bears Chengjiang fossils is the Yu'anshan Member (Cambrian unnamed stage 3), which together with the underlying Shiyantou Member (Cambrian unnamed stage 2) comprises the clastic lithostratigraphic unit known as the Chiungchussu Formation of the lower Cambrian of eastern Yunnan Province, China (Table 1). Within the literature, lithostratigraphic nomenclature is quite confusing, different authors having used different names (such as the Qiongzhusi Fm., Heilinpu Fm., Yu'anshan Fm., etc.). To help clarify this matter, we review changes of this lithostratigraphic unit's name (Table 1). Although the lithostratigraphic range of the Chiungchussu Formation was debated during the 1940s to 1970s, more recently it has been widely accepted that this formation is characterized by clastic deposition, with the upper member dominated by claystone (Yu'anshan Member) and the lower member dominated by siltstone (Shiyantou Member) (Luo et al., 1994). The Chiungchussu Formation was erected by Lu in 1941 (Lu, 1941), and was later updated as Qiongzhusi after the Chinese government formalized the phonetic symbol of Chinese in the 1950s. Subsequently, Qiongzhusi was adopted as the name of the second stage of the lower Cambrian (Qiongzhusian) when geologists began to establish a Chinese local chronostratigraphic system (reviewed by Luo et al., 1984, 1994). These two shifts clearly conflict with the priority rules of the *International Stratigraphic Guide*, and are thus invalid. The two members of the Chiungchussu Formation (Yu'anshan and Shiyantou) have also been elevated to formation level by Chen et al. (1997) but without any scientific reasoning being presented. From 2008, the National Commission on Stratigraphy of China (NCSC) began to revise Chinese local stratigraphic units (Wang et al., 2014). The name Chiungchussu Formation and its two subunits Yu'anshan and Shiyantou Members are accepted as valid (NCSC, 2012, 2014). Dozens of sections of Chengjiang fossils have been reported from the Chiungchussu Formation in the eastern part of Yunnan, and details of the localities can be found in Hou et al. (2004).

Articulated specimens of radiodontans from the Chengjiang biota are very rare. Fewer than 10 have been reported, though they represent almost all known Chengjiang species of radiodontans, including *Anomalocaris saron* (Chen et al., 1994; Hou et al., 1995), *Amplectobelua symbrachiata* (Chen et al., 1994),

Table 1. Historical nomenclature of the lithostratigraphic units of the Chiungchussu Formation, lower Cambrian, Eastern Yunnan, China.

Cambrian Global standard	Terreneuvian (part)	Series 2 (part)
	Stage 2 (part)	Stage 3 (part)
Chinese Stage	Meishucunian (part)	Nangaoan (part)
Lu, 1941	Chiungchussu Fm.*	
Luo, 1982	Qiongzhusi Fm.	
	Badaowan Mb.	Yu'anshan Mb.
Luo, 1990	Qiongzhusi Fm.	
	Shiyantou Mb.	Yu'anshan Mb.
Luo, 1994	Heilinpu Fm.	
	Shiyantou Mb.	Yu'anshan Mb.
Chen, 1997	Shiyantou Fm.	Yu'anshan Fm.
	4 unnamed members	*4 unnamed members*
NCSC, 2014	Chiungchussu Fm.	
	Shiyantou Mb.	Yu'anshan Mb.

(Left vertical label: **Historical terminology of lithostratigraphic units**)

*The lithostratigraphic range of Chiungchussu Lu, 1941 also included the underlying phosphate (*Hyolithes* layer of Lu, 1941).
NCSC, National Commission on Stratigraphy of China.

Parapeytoia yunnanensis, and *Cucumericrus decoratus* (Hou et al., 1995). All published material of these species was collected from the Chengjiang area, whereas recently reported articulated specimens of *Lyrarapax unguispinus* were collected from the Ercai and Mafang sections in the Haikou area of Kunming (Cong et al., 2014). Two new articulated specimens described in this paper were recently collected from the adjacent Jianshan section in the Haikou region (see Hu, 2005 for the detailed locality). The specimens were prepared with fine needles under high magnification on a Nikon SMZ1000 stereomicroscope, and photographed with a Nikon D3X digital camera or a Leica DFC 500 digital camera mounted to a Leica M205-C stereoscope under polarized and low-angle light. Interpretative drawings are based on camera lucida drawings and photographic evidence, and all images were processed in Adobe Photoshop CS5.

Repository and institutional abbreviation.—All specimens are deposited in the Yunnan Key Laboratory for Palaeobiology (YKLP), Yunnan University, Kunming, China.

Systematic paleontology

Phylum Euarthropoda Lankester, 1904
Order Radiodonta Collins, 1996

Emended diagnosis.—Bilaterally symmetrical, elongate arthropods with a nonmineralized cuticle typically most robust in the frontal appendages and possibly the circumoral structures. Body subdivided into two tagmata, a cephalic region with a pair of frontal appendages, a pair of eyes on stalks, a dorsal plate, and a radial circumoral structure and a metameric body with 10–14 segments bearing laterally directed flaps. Frontal appendages with at least six sclerotized podomeres separated by flexible arthrodial membranes and bearing single or paired ventral spines. Eyes compound and relatively large with stalk nearly as thick as visual surface; cephalic plate covering the dorsal surface of the head between the eyes of highly variable morphology. Ventral mouth with circumoral structures consisting of either plates or concentric furrows. Metameric body region with each segment bearing one or two pairs of imbricated, triangular flaps with associated setal blade structures consisting of parallel-oriented, elongated lanceolate blades (modified from Collins, 1996).

Remarks.—As the name suggests, the main diagnostic feature of Radiodonta originally was the presence of radial circumoral tooth-like plates. The new specimens of *Lyrarapax* described here show that the plated mouthparts are not necessarily present in all members of the group, as some only have circumoral furrows. Other diagnostic features of the body (metameric body with flaps and lanceolate blades, head with eyes on stalks and pair of frontal appendages bearing ventral spines) allow *Lyrarapax* to be included in Radiodonta despite the lack of circumoral plates.

Genus *Lyrarapax* Cong, Ma, Hou, Edgecombe and
Strausfeld, 2014

Type species.—*Lyrarapax unguispinus* Cong et al., 2014 from the Chengjiang biota, eastern Yunnan Province, China, by original designation.

Diagnosis.—Radiodontan with a pronounced, four-segmented neck; the head bears an oval to subcircular dorsal plate; mouth sub-circular to quadratic in outline, characterized by concentric wrinkled furrows; frontal appendage short, with a proximal podomere bearing a stout, blade-shaped endite with pectinate, sclerotized spines that gradually become larger distally; body flap of first trunk segment larger than succeeding body flaps.

Lyrarapax trilobus new species
Figures 1, 2, 3.1, 3.3

Types.—Holotype, YKLP 13322. Paratype, YKLP 13321a, b. Two known specimens held by Yunnan Key Laboratory for Palaeobiology, collected from Jianshan section, Yu'anshan Member, Chiungchussu Formation, Haikou area, Kunming, Yunnan Province.

Diagnosis.—*Lyrarapax* with a narrow body axis defined by two longitudinal furrows that extend from immediately behind head region to posterior part of trunk; frontal appendage composed of 11 podomeres, with endites only on odd numbered podomeres from the third onwards; endite of podomere 3 blade-shaped, bearing pectinate spines; small endite also present on second podomere but absent on first; body flap of the first trunk segment largest, with succeeding flaps narrowing gradually; trunk flaps bearing strengthening rays confined to the anterior part of the flap.

Occurrence.—Cambrian Series 2, Stage 3, Yu'anshan Member, Chiungchussu Formation (eastern Yunnan Province, China).

Etymology.—*trilobus* (Latin): referring to the trilobed appearance of the body of the new species imparted by the longitudinal furrows delineating the main body region.

Description.—The body of *Lyrarapax trilobus* includes a head region, a neck and a trunk region bearing a series of lateral flaps. Its size is similar to that of *L. unguispinus*. Paratype YKLP 13321 is approximately 4 cm from the anterior of the dorsal cephalic plate to the posterior end of the trunk (excluding a tail fan, if that structure is present) (Fig. 1.1–1.3), whereas holotype YKLP 13322 might have been up to 6 cm long, estimated from the size of its neck and first two trunk flaps (Fig. 2.4, 2.5).

The head bears a pair of frontal appendages, a pair of stalked eyes, a ventral mouth and a dorsal plate. The dorsal plate is the most anterior structure of the head, as illustrated in YKLP 13321 (Figs. 1.1–1.3, 2.1–2.3). It is oval to subcircular in shape, and has a thickened marginal rim at least in the anterior region. The stalked eyes are located lateral and slightly posterior to the dorsal plate. The frontal appendages are the most anterior ventral structure, with the poorly preserved ventral mouth located just posterior to them.

The paired frontal appendages of *Lyrarapax trilobus* are only known from YKLP 13322 (Figs. 2.4, 2.5, 3.1, 3.3), where

they are complete and twisted toward the left side of head at their basal attachment, with the left appendage parallel to and overlying the right one. This twisting causes the endites, which are located at the inner lateral side of the frontal appendages, to point towards anteriorly. This is more likely a result of taphonomy, e.g., transportation, rather than reflecting the life position of the appendages. The left appendage is preserved nearly straight, with curvature confined to the three most distal podomeres (Fig. 3.5). The appendage is just over 2 cm long. In total, 11 podomeres are known, with podomeres 3–11 visible on the left appendage, and podomeres 1–3 visible on the right appendage (Fig. 2.5). Podomere 3 has a remarkably stout endite, forming a spinose blade, on which there are up to 8 distally directed, sclerotized spines that gradually increase in length distally (Fig. 3.1, 3.3). From this podomere onward, only the odd podomeres (5, 7, 9, and 11) bear endites, these having a simple spine morphology (Fig. 3.5). These spines are paired, as indicated by the two spines visible on the endite of podomere 7 (Fig. 2.5). Podomeres 8 to 11 each have a small dorsal spine protruding anteriorly from the distal corner of the podomere (Figs. 2.5, 3.1, 3.6). A stout spinose endite can be observed on what is interpreted as podomere 3 of the right frontal appendage (Figs. 2.5, 3.3). The more distal region of the right appendage is embedded within sediment and overlain by the left appendage. A small endite with simple spine morphology is visible on podomere 2 of the right appendage, and podomere 1 has an elongated rectangular shape and lacks endites (Figs. 2.5, 3.1). The hint of a long spine can be recognized in the left appendage, crossing through the boundary of podomeres 4 and 5. The nature of this structure is unknown (Fig. 2.5).

A pair of subcircular-to-oval eyes is visible in both specimens, each attached at the distal end of a stout stalk. The stalks are preserved bent slightly backwards, positioning the eyes beside the neck (Figs. 1.1, 1.2, 2.1, 2.2, 2.4, 2.5). In YKLP 13322, the remains of retinal pigmentation form a subcircular black area in each eye (Fig. 2.4, 2.5). At the boundary between the right eye and its stalk, several transverse wrinkles are visible. Similar wrinkles also occur in the right eye of YKLP 13321b, whereas in the left concentric wrinkles can be observed, indicating that originally the eyes were convex (Fig. 2.1, 2.2).

In the mouth region of YKLP 13322, mineralization occurs as an irregular dark shape, but no sign of the oral cone can be identified (Fig. 2.4, 2.5). In the same area of YKLP 13321, there are concentric lines that form a subsquare shape (Figs. 1.3, 1.5, 2.2, 2.3). This is interpreted as the mouth, similar to the oral opening of *Lyrarapax unguispinus* (Cong et al., 2014, fig. 1), which is also encircled by a series of wrinkles and furrows.

The trunk of *Lyrarapax trilobus* includes a four-segmented neck region and a main body bearing flaps. As in *L. unguispinus*, the neck is located immediately behind the head, comprising four reduced flaps. The fourth neck flap is overlapped by the first body flap (Figs. 1.3, 1.5, 2.2). In YKLP 13321a, a total of 10 body flaps can be recognized on the right side of the body (Fig. 1.1–1.3), indicating that the body of *L. trilobus* has at least 10 body segments in addition to four neck segments. The first pair of body flaps are the widest, and the succeeding flaps decrease in size posteriorly in a regular fashion. Unlike *L. unguispinus*, the first pair of body flaps is not significantly wider than the succeeding ones.
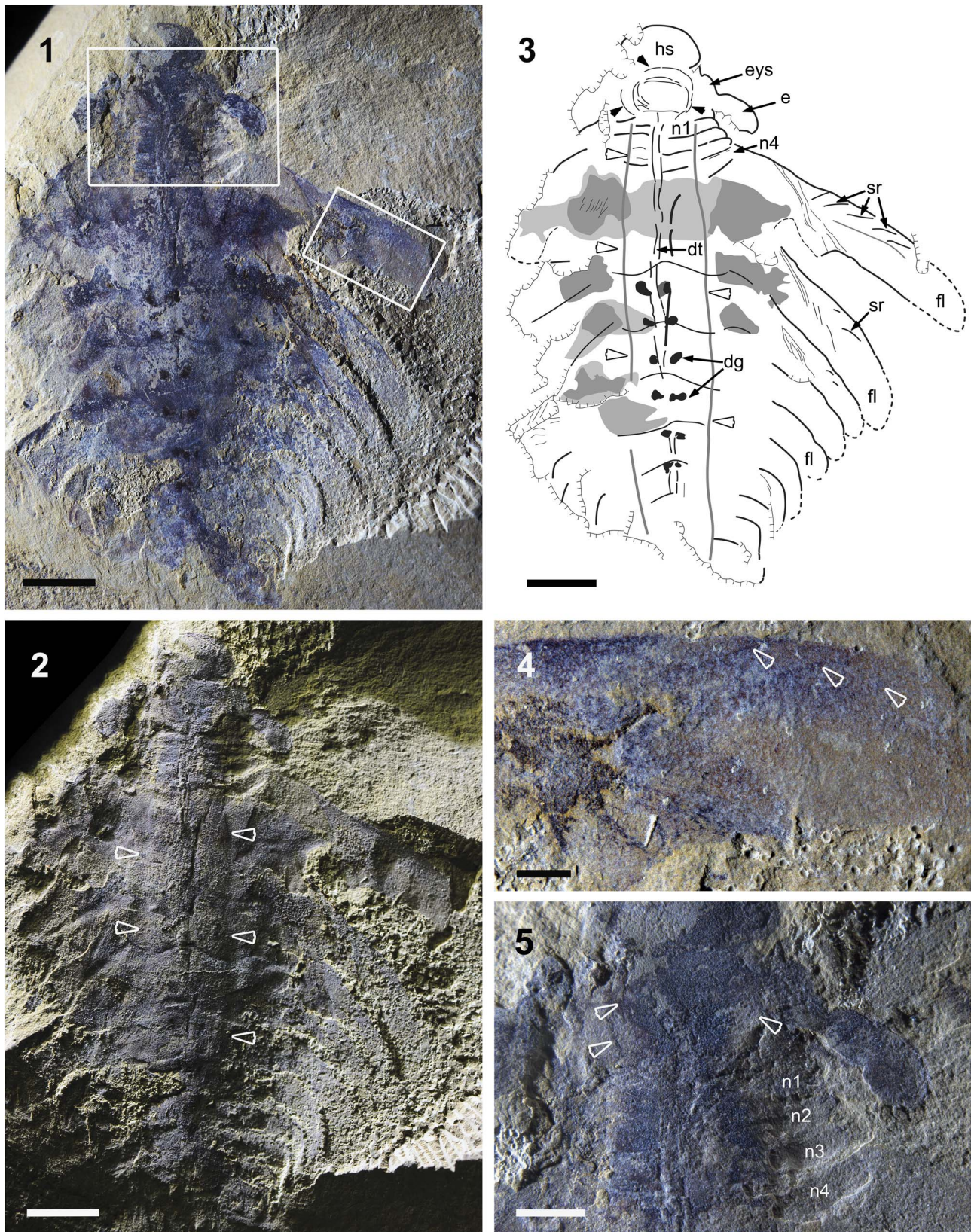
Figure 1. *Lyrarapax trilobus*, n. sp. YKLP 13321a, Cambrian Stage 3, Chengjiang bioa, China. (**1**) Photographed with polarized light, boxed areas indicate close-up of (**4**) (right) and (**5**) (top); (**2**) photographed with low-angle light, arrowheads indicate furrows that divide the body into three lobes. (**3**) Interpretive drawing, concentric lines of mouth are indicated by solid arrows, body furrows indicated by hollow arrows; the gray regions show possible remains of setal blades and muscles. dg, digestive glands; dt, digestive tract; e, eyes; eys, eye stalk; fl, flap; hs, head segment; n, neck segment; sr, strengthening ray. (**4**) Close-up of first right trunk flap, with strengthening rays indicated by arrowheads. (**5**) Close-up of neck region, with concentric lines of mouth indicated by arrowheads. n, neck segment. Scale bars represent (**1–3**) 5 mm, (**4**) 1 mm, (**5**) 2 mm.
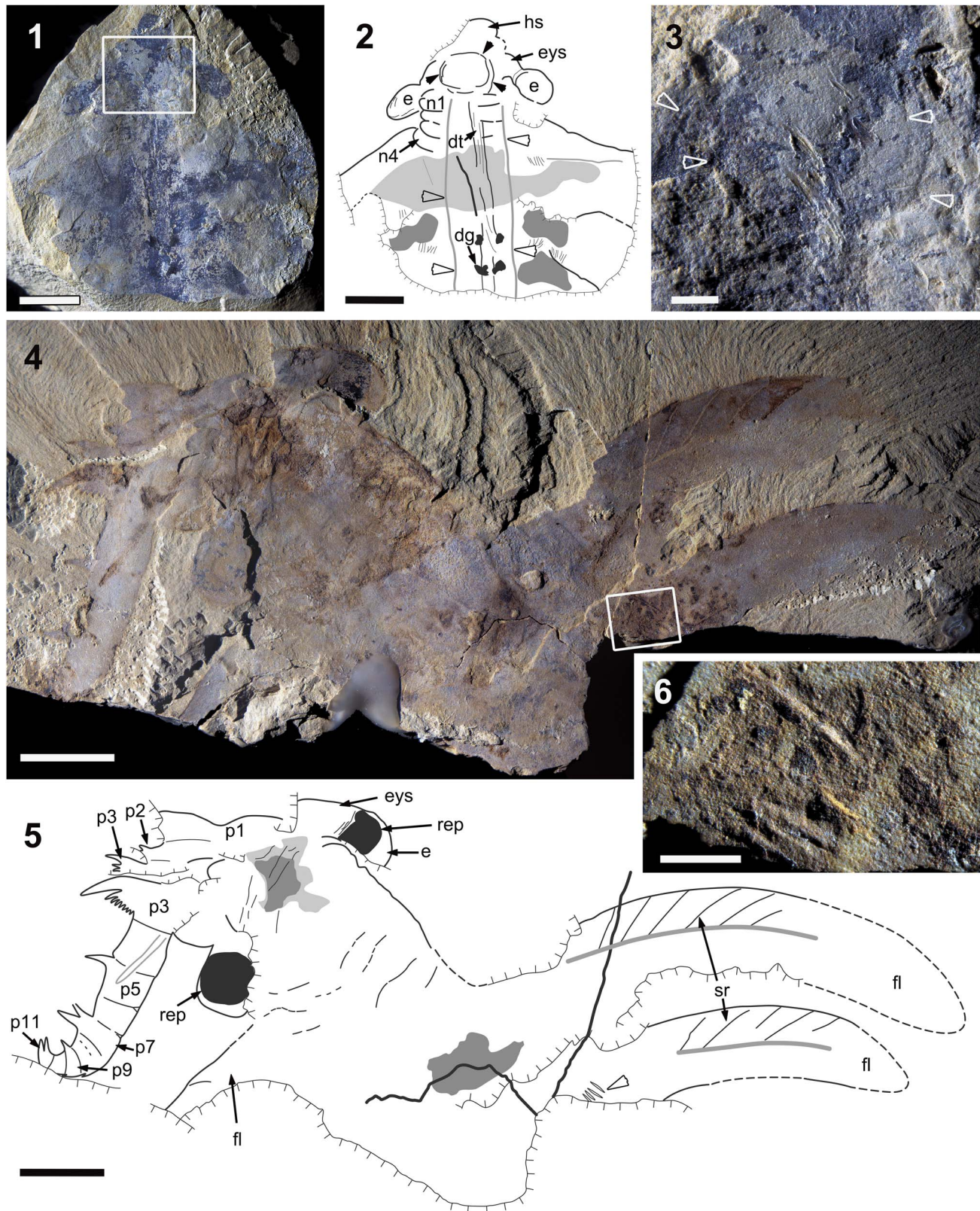
Figure 2. *Lyrarapax trilobus* n. sp. from the Chengjiang biota. (**1–3**) YKLP 13321b; (**1**) photographed with polarized light, boxed area indicates close-up of (**3**). (**2**) Interpretive drawing, concentric lines of mouth are indicated by solid arrowheads, body furrows indicated by open arrowheads; the gray region shows possible remains of setal blades and muscles. dg, digestive glands; dt, digestive tract; e, eyes; eys, eye stalk; hs, head segment; n, neck segment. (**3**) Close-up of mouth region showing concentric lines (arrowheads). (**4–6**) YKLP 13322, holotype; (**4**) photographed with polarized light, boxed area indicates close-up of (**6**). (**5**) Interpretive drawing, mouth region indicated by gray (between the eyes); another gray region at the proximal part of flaps interpreted as possible remains of setal blades and muscles. e, eyes; eys, eye stalk; fl, flap; p, podomere of frontal appendage; rep, remains of retinal pigmentation; sr, strengthening ray. (**6**) Close-up of high-relief linear structures. Scale bars represent (**1, 2**) 5 mm, (**3, 6**) 0.5 mm, (**4, 5**) 1 cm.
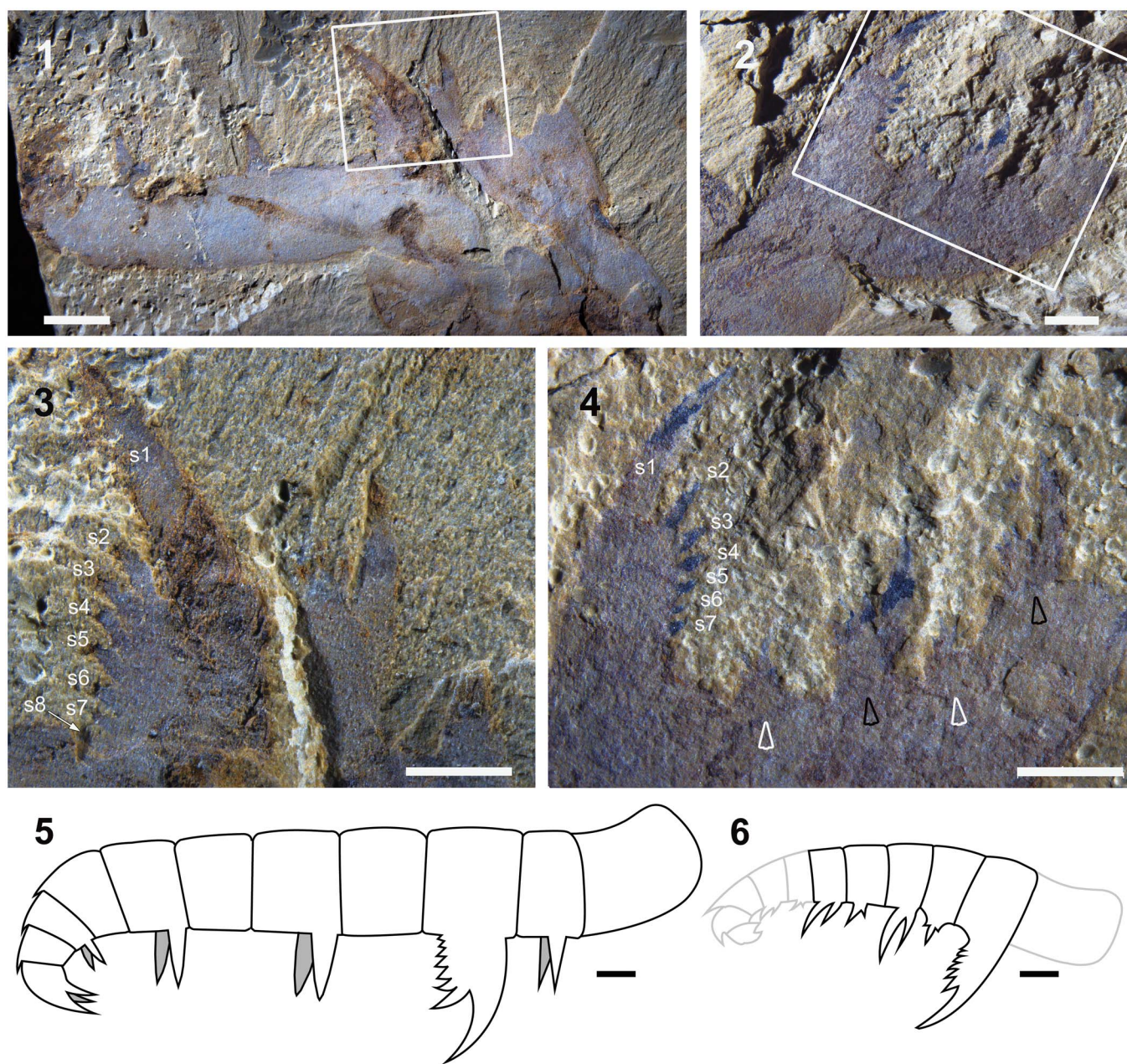
Figure 3. Comparison of the frontal appendages of *Lyrarapax trilobus* n. sp. and *L. unguispinus*. (**1**) Frontal appendage of *L. trilobus* (YKLP 13322), boxed area indicates close-up of (**3**). (**2**) Frontal appendage of *L. unguispinus* (YKLP 13304), boxed area indicates close-up of (**4**). (**3**) Close-up of the blade-shaped spinose endite in (**1**), s1–s8 indicate the spines on this endite. (**4**) Close-up of the blade-shaped spinose endite in (**2**), s1–s7 showing spines on this endite; note the endites on other podomeres are also spinose and their size changes alternatively (arrowheads). (**5**, **6**) Frontal appendage reconstructions drawn to scale for (**5**) *L. trilobus* and (**6**) *L. unguispinus*. Scale bars represent (**1**) 2 mm, (**2–6**) 1 mm.

Strengthening rays (Whittington and Briggs, 1985), veins (Chen et al., 1994; Hou et al., 1995) or transverse lines (Daley et al., 2013b; Daley and Edgecombe, 2014) can be recognized in the first two pairs of body flaps both in YKLP 13321 (Fig. 1.3, 1.4) and YKLP 13322 (Fig. 2.4, 2.5). They start from the anterior margin of the flap and extend only as far as the flap center. In the first body flap of YKLP 13322, the anterior part that bears the transverse lines has a darker coloration than the posterior region, between which a separating line can be determined (Fig. 2.4, 2.5). The angle between the transverse line and the anterior margin of the flap varies between less than 30° to over 45° and is normally larger near the proximal part of the flap. In the first body flap of YKLP 13321, the angle is approximately 20°, which might be caused by deformation of the flap (Fig. 1.1, 1.3). The third body flap of YKLP 13321 also bears traces of transverse lines, suggesting that all body flaps may have had these structures (Fig. 1.1, 1.3).

Pairs of patches with darker coloration can be recognized in each body segment extending into the proximal region of the flaps (Figs. 1.1, 1.3, 2.1, 2.2), with a similar preservation to the carbon-rich organ system(s) seen in *Lyrarapax unguispinus* (Cong et al., 2014) but with a less regular morphology and size.

On the left side of the body of YKLP 13321a, these patches have clear edges and normally curve outward from the central body axis, ending at the proximal part of the flaps (Fig. 1.1, 1.3), indicating that they might represent the edge of either setal blades or musculature. On the right side of YKLP 13322, a similar patch with dark coloration can be recognized at the most basal part of the first body flap (Fig. 2.4, 2.5).

The basal region of the second body flap on the right side of YKLP 13322 bears several high relief linear structures (Fig. 2.4–2.6) similar to structures observed in *Anomalocaris canadensis* (Daley and Edgecombe, 2014, figs. 5, 6.1, 6.3, 6.4, 9.3). These are no more than 0.1 mm wide and 1.5 mm long, and the long axis oriented roughly parallel to the anterior-posterior axis of the body. They are generally straight with uneven but close spacing between them, and no clear connections linking each individual element. The high relief linear structures seem to be located midway between the anterior and posterior margin of the flap, although a break in the rock makes it difficult to determine if they would have been located in the overlap region between successive flaps.

A narrow tube-like structure extends anteroposteriorly from directly behind the mouth to the posterior of the body (Figs. 1.1–1.3, 2.1, 2.2). This structure is interpreted as the gut, and has a consistent width from anterior to posterior. Immediately beside the gut, a pair of small, roughly circular, black patches is distinct in each of trunk segments 2 to 7 (Figs. 1.1, 1.3, 2.1, 2.2). These six pairs of patches are interpreted as digestive glands, owing to their position adjacent to the gut and their similar preservation and morphology to the gut glands of other radiodontans (Daley and Edgecombe, 2014, MD in fig. 7.2).

Two broad anteroposteriorly extended furrows can be observed with very low angle lights in YKLP 1331 (Fig. 1.2), dividing the trunk into three lobes with the central region being convexly raised as compared to the lateral regions. The furrows start anteriorly at the base of the head, pass through the neck region and most of the body, and start to narrow from body segment 8 onward. The axial region has a similar width in the neck and through most of the main body.

Remarks.—Although the new species closely resembles *Lyrarapax unguispinus*, a few features permit these two taxa to be distinguished from each other. The main difference is in the morphology of the frontal appendages (Fig. 3). In the new species, the endites are present only on alternating podomeres (Fig. 3.5), whereas *L. unguispinus* has endites on every podomere that alternate between large and small sizes (Fig. 3.6). Additionally, the podomere shapes are very different between the two taxa. Specimen YKLP 13322 of the new species shows that the podomeres are elongated along the proximal-distal axis of the appendage (Fig. 3.5), giving it an overall elongated appearance as compared to *L. unguispinus* in which the podomeres are shorter in the proximal-distal axis, and relatively narrower (Fig. 3.6). A final possible difference between the appendages is that *L. trilobus* has its large stout endite on podomere 3 (Fig. 3.5), whereas *L. unguispinus* has this structure on podomere 2 (Fig. 3.6), such that the new speices has an extra proximal endite-bearing podomere, but it cannot be ruled out that the absence of this structure in *L. uniguispinus* is a

taphonomic artifact. Another difference between the two *Lyrarapax* species is that the new species has transverse lines located on the anterior margin of the flaps (Figs. 1.4, 2.4, 2.5), whereas *L. uniguispinus* has the anterior margin of its large posterior flap covered in fine striations (Cong et al., 2014, extended data fig. 3c).

Discussion

Access to new material of the rare radiodontan *Lyrarapax* allows several morphological and taxonomic questions about this genus to be clarified. These include details of the frontal appendages, gut anatomy, body flaps, and general trunk morphology, as well as the mouth apparatus.

Frontal appendage morphology provides the main differences between *Lyrarapax unguispinus* and *L. trilobus* (Fig. 3). Although the frontal appendage of *L. unguispinus* is incomplete (Cong et al., 2014), its distal end being unknown, its partial preservation still clearly shows that it differs from *L. trilobus* in diagnostic ways. The podomere shape of *L. trilobus* imparts an elongated nature to this frontal appendage that is similar to that of *Anomalocaris saron* (Hou et al., 1995), whereas the narrow podomeres in *L. unguispinus* resemble *Amplectobelua symbrachiata* (Hou et al., 1995). Although both *Lyrarapax* species and *Amplectobelua* have an enlarged endite, only the former have their enlarged endite adorned with at least seven robust spines. *Anomalocaris saron* has multiple pairs of spines on its ventral endites, but it lacks the enlarged endite that is present in *Lyrarapax* and *Amplectobelua*. The Chengjiang radiodontan frontal appendages all have their distinct characteristics and do not represent morphological gradients, ontogenetic variants or taphomorphs. Ontogeny is unlikely to explain the difference between the two species of *Lyrarapax* because the estimated body lengths of the most complete specimens of both *L. trilobus* (YKLP13321) and *L. unguispinus* (YKLP13305, Cong et al., 2014, fig. 2a, b) are approximately the same (4 cm). Ontogenetic series for frontal appendages (e.g., Cong et al., 2014, extended data Fig. 1 for *Amplectobelua symbrachiata*) indicate that species-level characters are consistent within the size difference of the known appendages of *L. trilobus* and *L. unguispinus* (Fig. 3).

Midgut glands were not previously recognized in *Lyrarapax*, not being visible in the three previously available specimens of *L. unguispinus* (Cong et al., 2014). The new material documented herein demonstrates their presence in *L. trilobus*, indicating that they occur in this genus. Likewise, the absence of strengthening rays/transverse lines on the trunk flaps in *L. unguispinus* was a rather unexpected character state, given their widespread presence in radiodontans. These structures are clearly visible in *L. trilobus*, showing that their absence is not a typical character of the genus as a whole. Re-examination of *L. unguispinus* shows that the anterior margin of the flaps in this species is covered in striations rather than transverse lines (Cong et al., 2014, extended data fig. 3c). While the transverse lines of *L. trilobus* are most similar to those seen in *Anomalocaris saron* (Chen et al., 1994, figs. 1, 2; Hou et al., 1995, figs. 4–6) and *Amplectobelua symbrachiata* (Chen et al., 1994, fig. 3c), the striations in *L. unguispinus* resembles the striations on the flaps of *Anomalocaris canadensis* (Daley and Edgecombe, 2014, figs. 1, 2, 4.4). Ornamentation of

the flaps appears to be a highly variable characteristic within Radiodonta.

The high relief linear structures described here for *Lyrarapax trilobus* represent the first documented observation of this feature in a taxon other than *Anomalocaris canadensis* (Daley and Edgecombe, 2014). These features were suggested to provide structural support by attaching adjacent body flaps together and stabilizing them against shearing action as the animal moved to create forward propulsion. This argument was based on the placement of these features in the region where adjacent flaps overlap one another. The incompleteness of the only *Lyrarapax* specimen showing these features does not allow us to confidently confirm a similar placement in this taxon, but their identification suggests that high-relief linear structures could be widely present within radiodontans but are preserved only rarely.

A hypertrophied anterior trunk flap in *Lyrarapax unguispinus* was considered to be diagnostic for the genus by Cong et al. (2014). This drew especially on specimen YKLP 13305 (Cong et al., 2014, fig. 2), in which the first flap appeared to be much larger than the second and subsequent flaps. *L. trilobus* shows that the body is indeed widest across the first flap but it has a more gradational narrowing than appeared to be the case in *L. unguispinus*. We consider it likely that only the basal parts of the second and more posterior flaps are preserved in YKLP 13305, their distal edges being associated with a break in slope suggesting fragmentation. If this reinterpretation is correct, then the "hypertrophied" first flap should be discarded as diagnostic. This brings *Lyrarapax* more in line with the general body morphology of radiodontans.

Lyrarapax trilobus uniquely preserves a trilobed aspect to the body, with a raised central body region being separated from the laterally oriented flaps by a distinct margin (arrows in Fig. 1.2). Although interpretation of the body architecture of radiodontans has historically been widely debated (Whittington and Briggs, 1985; Bergström, 1986, 1987; Collins, 1996; Daley et al., 2009), recent descriptions are converging on a morphology that appears to be common to all taxa from which body specimens are known (e.g., Daley and Edgecombe, 2014; Van Roy et al., 2015) and is most similar to the configuration described for *Peytoia* by Bergström (1986, 1987). This consists of a rounded central body core that contains the gut structures and has a convex relief that is much higher than the relatively flat flaps, which extend out laterally and are attached to the ventral region of the main body core. Attachment of the setal blades is either directly to the central body core in taxa such as *Anomalocaris canadensis* (Daley and Edgecombe, 2014) and *Peytoia nathorsti* (Daley et al., 2009), or at the base of the flaps (and extending over the dorsal surface of the body core) in taxa such as *Hurdia victoria* and *Aegirocassis benmoulae* (Van Roy et al., 2015). The raised central body region seen in specimen YKLP 13321a of *L. trilobus* may be a partial three-dimensional preservation of the original body relief, showing the raised central body core and the flatter, laterally oriented flaps. In this specimen, the gut structures are confined to this body region, but areas of darkened mineralization extend beyond its margins onto the surrounding flaps. This mineralization likely represents either musculature or setal blades, but the lack of preservation of fine details in this taxon makes it impossible to determine which. Areas of well-preserved musculature are found in a similar

location in *L. unguispinus* (Cong et al., 2014, figs. 1a–d, 2a–e). Setal blade preservation in general in *Lyrarapax* is poor, but it may be that in this genus they are not confined to a location on the dorsal surface of the central body core, given that small patches of setal blades have been described at the bases of body flaps six and seven in one specimen of *L. unguispinus* (Cong et al., 2014, extended data fig. 3a, d, e). Exact description of the details of the body architecture of *Lyrarapax* awaits further specimens, but its general aspect seems to conform to that seen in other radiodontans.

Especially informative is the discovery that this second *Lyrarapax* species also preserves the mouth apparatus and shows it to consist of concentric furrows (Cong et al., 2014), rather than the sclerotized plates seen in all other known radiodontans (Daley and Bergström, 2012). This suggests that the lack of circumoral plates in *L. unguispinus* was not owing to taphonomic loss, but represents the true morphology of circumoral structures in this genus. Oral cones are generally not well preserved in the Chengjiang biota as compared to the hundreds of known frontal appendages. Described specimens of Chengjiang oral cones consist of only two more or less in situ oral cones of *Anomalocaris saron* (ELRC 20001 in Chen et al., 1994 and NIGPAS 115341 in Hou et al., 1995), a partial isolated specimen from *Anomalocaris* (ELRC 22020b in Chen et al., 1994), and possible plates associated with a full-body specimen (ELRC 21001 in Chen et al., 1994) or frontal appendages (NIGPAS 115346 in Hou et al., 1995) of *Amplectobelua symbrachiata*. Oral cones from the Burgess Shale are abundant, and a recent examination of their morphology revealed that the oral cone of *Anomalocaris canadensis* was less sclerotized and more irregular than the typical tetraradial oral cones of taxa such as *Peytoia* and *Hurdia* (Daley and Bergström, 2012). This was already hinting that oral cone morphology was more variable than previously assumed, and the circumoral furrows of *Lyrarapax* extend this variability even further.

The lack of sclerotized oral cone plates in *Lyrarapax* forced us to revisit the diagnosis of the order Radiodonta. As originally described, the major diagnostic criterion was the presence of a sclerotized oral cone with plates (Collins, 1996) but *Lyrarapax* shows us that this is not a trait shared by all radiodontans. Furthermore, the gilled lobopodian *Pambdelurion* (Budd, 1998), which falls outside the radiodontan clade in phylogenetic analyses (Daley et al., 2009; Legg et al., 2013; Cong et al., 2014; Smith and Ortega-Hernández, 2014; Van Roy et al., 2015), has an irregular arrangement of sclerotized plates surrounding its mouth, in some respects more similar to radiodontans than the circumoral structures of *Lyrarapax*. Accordingly, if *Lyrarapax* is a radiodontan (as is strongly indicated by its dorsal cephalic plate, frontal appendage structure, body flaps with strengthening rays, etc.), the diagnostic characteristics of Radiodonta must extend beyond the oral cone morphology. Given that the general body morphology with swim flaps extending laterally from the body is not unique to the radiodontans, because flaps are also found in *Pambdelurion* (Budd, 1998), the robust raptorial frontal appendages become the key characteristic uniting Radiodonta. Radiodontan frontal appendages are distinct from the paired anteriormost appendages of arthropod taxa found further crownward (fide the phylogeny of Legg et al., 2013), such as the megacheirans (Hou and Bergström, 1997; Edgecombe et al., 2011, Aria et al., 2015), in having more than six podomeres and

always having at least one row of ventral spines that usually bear a second order of spinosity. We have emended the diagnosis of Radiodonta to reflect these observations.

The description of a new species of *Lyrarapax* continues to build on the increasing diversity of radiodontans described recently for other sites in China (Huang et al., 2012; Liu, 2013; Cong et al., 2014) and around the world (Daley and Budd, 2010; Daley et al., 2013b; Vinther et al., 2014; Lerosey-Aubril et al., 2014; Van Roy et al., 2015). As the most abundantly preserved and robust feature of the anatomy, frontal appendages are again shown here to provide key diagnostic features on which to base radiodontan systematics.

Acknowledgments

References

Aria, C., Caron, J., and Gaines, R., 2015, A large new leanchoiliid from the Burgess Shale and the influence of inapplicable states on stem arthropod phylogeny: Palaeontology, v. 58, p. 629–660.

Bergström, J., 1986, *Opabinia* and *Anomalocaris*, unique Cambrian 'arthropods': Lethaia, v. 19, p. 241–246.

Bergström, J., 1987, The Cambrian *Opabinia* and *Anomalocaris*: Lethaia, v. 20, p. 187–188.

Budd, G.E., 1993, A Cambrian gilled lobopodian from Greenland: Nature, v. 364, p. 709–711.

Budd, G.E., 1998, Arthropod body-plan evolution in the Cambrian with an example from anomalocaridid muscle: Lethaia, v. 31, p. 197–210.

Chen, J., Ramsköld, L., and Zhou, G., 1994, Evidence for monophyly and arthropod affinity of Cambrian giant predators: Science, v. 264, p. 1304–1308.

Chen, J., Zhou, G., Zhu, M., and Yeh, K., 1997, The Chengjiang Biota, A Unique Window of the Cambrian Explosion, Taichung, National Museum of Natural Science, 222 p. [in Chinese].

Collins, D., 1996, The "evolution" of *Anomalocaris* and its classification in the arthropod class Dinocarida (nov.) and order Radiodonta (nov.): Journal of Paleontology, v. 70, p. 280–293.

Cong, P., Ma, X., Hou, X., Edgecombe, G.D., and Strausfeld, N.J., 2014, Brain structure resolves the segmental affinity of anomalocaridid appendages: Nature, v. 513, p. 538–542.

Daley, A.C., and Bergström, J., 2012, The oral cone of *Anomalocaris* is not a classic "peytoia": Naturwissenschaften, v. 99, p. 501–504.

Daley, A.C., and Budd, G.E., 2010, New anomalocaridid appendages from the Burgess Shale, Canada: Palaeontology, v. 53, p. 721–738.

Daley, A.C., and Edgecombe, G.D., 2014, Morphology of *Anomalocaris canadensis* from the Burgess Shale: Palaeontology, v. 88, p. 68–91.

Daley, A.C., and Peel, J.S., 2010, A possible anomalocaridid from the Cambrian Sirius Passet Lagerstätte, North Greenland: Journal of Paleontology, v. 84, p. 352–355.

Daley, A.C., Budd, G.E., Caron, J.-B., Edgecombe, G.D., and Collins, D., 2009, The Burgess Shale anomalocaridid *Hurdia* and its significance for early euarthropod evolution: Science, v. 323, p. 1597–1600.

Daley, A.C., Budd, G.E., and Caron, J.-B., 2013a, The morphology and systematics of the anomalocaridid *Hurdia* from the Middle Cambrian of British Columbia and Utah: Journal of Systematic Palaeontology, v. 11, p. 743–787.

Daley, A.C., Paterson, J.R., Edgecombe, G.D., García-Bellido, D.C., and Jago, J.B., 2013b, New anatomical information on *Anomalocaris* from the Cambrian Emu Bay Shale of South Australia and a reassessment of its inferred predatory habits: Palaeontology, v. 56, p. 971–990.

Edgecombe, G.D., García-Bellido, D.C., and Paterson, J.R., 2011, A new leanchoiliid megacheiran arthropod from the Lower Cambrian Emu Bay Shale, South Australia: Acta Palaeontologica Polonica, v. 56, p. 385–400.

Hou, X., and Bergström, J., 1997, Arthropods of the Lower Cambrian Chengjiang fauna, southwest China, Fossils and Strata, No. 45 116 p.

Hou, X., Bergström, J., and Ahlberg, P., 1995, *Anomalocaris* and other large animals in the Lower Cambrian Chengjiang Fauna of southwest China: GFF, v. 117, p. 163–183.

Hou, X., Aldridge, R.J., Bergström, J., Siveter, D.J., Siveter, D.J., and Feng, X., 2004, The Cambrian fossils of Chengjiang, China - the flowering of early animal life, Oxford, Blackwell Science, xii + 233p.

Hu, S., 2005, Taphonomy and palaeoecology of the Early Cambrian Chengjiang biota from Eastern Yunnan, China: Berliner Paläobiologische Abhandlungen, band, v. 7, 197 p.

Huang, D., Wang, Y., Gao, J., and Wang, Y., 2012, A new anomalocaridid frontal appendage from the Middle Cambrian Mantou Formation of the Tangshan Area: Acta Palaeontologica Sinica, v. 51, p. 411–415 [in Chinese with English abstract].

Kühl, G., Briggs, D.E.G., and Rust, J., 2009, A great-appendage arthropod with a radial mouth from the Lower Devonian Hunsruck Slate, Germany: Science, v. 323, p. 771.

Lankester, E.R., 1904, The structure and classification of Arthropoda: Quarterly Journal of Microscopical Science, v. 47, p. 523–582.

Legg, D.A., Sutton, M.D., and Edgecombe, G.D., 2013, Arthropod fossil data increase congruence of morphological and molecular phylogenies: Nature Communications, v. 4, n. 2485 doi: 10.1038/ncomms3485.

Lerosey-Aubril, R., Hegna, T.A., Babcock, L.E., Bonino, E., and Kier, C., 2014, Arthropod appendages from the Weeks Formation Konservat-Lagerstätte: new occurrences of anomalocaridids in the Cambrian of Utah, USA: Bulletin of Geoscience, v. 89, p. 269–282.

Liu, Q., 2013, The first discovery of anomalocaridid appendages from the Balang Formation (Cambrian Series 2) in Hunan, China: Alcheringa, v. 37, p. 338–343.

Lu, Y., 1941, Lower Cambrian stratigraphy and trilobite faunas of Kunming, Yunnan: Bulletin of the Geological Society of China, v. 21, p. 71–90.

Luo, H., Jiang, Z., Wu, X., Song, X., Lin., O., Xing, Y., Liu, G., Zhang, S., and Tao, Y., 1984, Sinian-Cambrian Boundary Stratotype Section at Meishucun, Jinning, Yunnan, China, Kunming, People's Publishing House of Yunnan, 154 p. [In Chinese with English summary].

Luo, H., Jiang, Z., and Tang, L., 1994, Stratotype Section for Lower Cambrian Stages in China, Kunming, Yunnan Science and Technology Press, 183 p. [In Chinese with English summary].

National Commission on Stratigraphy of China (NCSC), ed., 2012, Stratigraphic Chart of China (English version), Beijing, Geological Publishing House.

National Commission on Stratigraphy of China (NCSC), ed., 2014, Stratigraphic Chart of China, Beijing, Geological publishing House [In Chinese].

Nedin, C., 1995, The Emu Bay Shale, a Lower Cambrian fossil Lagerstätten, Kangaroo Island, South Australia: Memoirs of the Association of Australian Palaeontologists, v. 18, p. 31–40.

Ortega-Hernández, J., 2015, Homology of head sclerites in Burges Shale euarthropods: Current Biology, v. 25, p. 1625–1633.

Paterson, J.R., García-Bellido, D.C, Lee, M.S.Y., Brock, G.A., Jago, J.D., and Edgecombe, G.D., 2011, Acute vision in the giant Cambrian predator *Anomalocaris* and the origin of compound eyes: Nature, v. 480, p. 237–240.

Smith, M.R., and Ortega-Hernández, J., 2014, *Hallucigenia*'s onychophoran-like claws and the case for Tactopoda: Nature, v. 514, p. 363–366.

Van Roy, P., and Briggs, D.E.G., 2011, A giant Ordovician anomalocaridid: Nature, v. 473, p. 510–513.

Van Roy, P., Daley, A.C., and Briggs, D.E.G., 2015, Anomalocaridid trunk limb homology revealed by a giant filter feeder with paired flaps: Nature, v. 522, p. 77–80.

Vinther, J., Stein, M., Longrich, N.R., and Harper, D.A.T., 2014, A suspension-feeding anomalocarid from the Early Cambrian: Nature, v. 507, p. 496–499.

Walcott, C.D., 1911, Middle Cambrian Holothurians and Medusae: Smithsonian Miscellaneous Collections, v. 57, p. 41–68.

Walcott, C.D., 1912, Middle Cambrian Branchiopoda, Malacostraca, Trilobita and Merostomata: Smithsonian Miscellaneous Collections, v. 57, p. 145–228.

Wang, Y., Huang, D., and Hu, S., 2013, New anomalocaridid frontal appendages from the Guanshan biota, eastern Yunnan: Chinese Science Bulletin, v. 58, p. 3937–3942.

Wang, Z., Huang, Z., Yao, J., and Ma, X., 2014, Characteristics and main progress of the Stratigraphic Chart of China and Directions: Acta Geoscientica Sinica, v. 35, p. 271–276 [In Chinese with English abstract].

Whiteaves, J.F., 1892, Description of a new genus and species of phyllocarid Crustacea from the Middle Cambrian of Mount Stephen, B.C.: Canadian Record of Science, v. 5, p. 205–208.

Whittington, H.B., and Briggs, D.E.G., 1985, The largest Cambrian animal, *Anomalocaris*, Burgess Shale, British Columbia: Philosophical Transactions of the Royal Society of London, Series B, v. 309, p. 569–609.